P2.41A CONTRAIL COVERAGE OVER WESTERN EUROPE
DERIVED FROM 2 YEARS OF NOAA-AVHRR-DATA

Richard Meyer*, Hermann Mannstein
Institut für Physik der Atmosphäre, DLR Oberpfaffenhofen

1 INTRODUCTION

High and optically thin ice clouds reduce the outgoing longwave flux at top of atmosphere mostly stronger than they decrease the downward solar radiative flux [13]. Thus an increase of thin ice clouds may lead to warmer surface temperatures [6].

Under certain atmospheric conditions aircraft form condensation trails [11] that can persist covering large proportions of the sky. In regions where these conditions for formation of persistent contrails are frequent and air traffic is dense the regional climate is affected. Due to the rapid growth of air traffic - fuel consumption is increasing 3 % per year [10] - its possible effects need further study.

To model the regional and global climatic effect of contrails we need to know their temporal and spatial distribution as well as their optical properties. Optical properties can be derived from in-situ measurements [4] and by remote sensing techniques [2, 5, 9]. Frequency can be obtained from synoptic observations of contrails as it was made by Minnis et al. [8] for the US, but to acquire their mean coverage of the sky areal measurements have to be taken. For this task we need remote sensing data with a high repetition rate and reasonable spatial resolution. Up to now only a few studies on regional contrail coverage have been performed. Mostly AVHRR data was used due to the availability of long time-series which is needed for proper means. Schumann and Wendling [12] estimate an average contrail coverage of 1.5 % from AVHRR-data for Southern Germany and the Alps. Bakan et al. [1] analyzed the biggest data set so far. Through visual inspection of daily AVHRR hard-copies from 52 months an average contrail coverage of 1 % over Central Europe and 2 % over the eastern part of the North Atlantic was obtained.

All these observations suffered from the subjectivity introduced by visual interpretation. Therefore there was a strong need for a fully automated scheme that detects contrails in satellite data. Engelstad et al. [3] created the first algorithm which was able to find contrails in AVHRR data, but had the tendency to misinterpret linear streaks of natural cirrus as contrails. The algorithm used here [7] was designed to have a low false alarm rate at a constant detection rate. This for the first time enables to analyze a large number of AVHRR-scenes operationally.

2 DETECTING CONTRAILS

With passive remote sensing methods ice clouds are recognized mainly by their low brightness temperatures in the thermal infrared. Due to originally smaller crystal sizes contrails [4] tend to show higher transmissivity in the AVHRR-channel 4 ($T4$: 10.3 to 11.3 μm) than in channel 5 ($T5$: 11.5 to 12.5 μm). This mostly causes contrails to appear bright on temperature difference images $TD = T4 - T5$.

The algorithm used here is described en detail by Mannstein et al. [7]. It takes advantage of both the mostly bright ridges contrails show in the TD-images and in the inverted temperature image $T5i$.

Unfortunately contrails often appear as very fuzzy structures hard to distinguish from background. Other objects like cloud edges, coast lines, mountain ridges etc. also form linear ridge structures of comparable scale and amplitude.

Therefore we take a scheme that combines different tests to avoid misdetections. Those tests are mainly based on spatial patterns - the way a human observer recognizes contrails in satellite images. Important for the derivation of climatological values is a constant detection efficiency for all scenes and viewing angles. To make the data independent from the individual scenery both images get normalized with their local standard deviation in a 5 x 5 surrounding ($\overline{SDTD}, \overline{SDT5}$). Within these normalized images the contrast is evenly distributed and independent from size and content of the actual scene. Therefore we can use global thresholds without loosing much sensitivity.

In the next step we use the sum of the normalized images N to avoid the interpretation of boundary layer cloud streets as contrails. To derive linear elements N is convolved with a line filter of 19 x 19 pixels in 16 different directions.

Because of the normalization of the input data, a single threshold is sufficient to isolate connected regions. These regions are treated as separate objects which might be contrails. Each of these objects is now checked against a binary mask which combines the following criteria:

$$N > 1.5, \quad (1)$$

$$TD > 0.2\text{K}. \quad (2)$$

$$\overline{G5} < 2 \cdot \overline{SDT5} + 1\text{K}, \quad (3)$$

where $\overline{G5}$ is the large scale maximum gradient for $T5$ calculated in a 15 x 15 pixel vicinity. Afterwards we recombine elongated structures disrupted by this check

*Corresponding author address: Deutsches Zentrum für Luft- und Raumfahrt e.V. (DLR), Institut für Physik der Atmosphäre, D-82234 Wessling; Tel +49 8153 28 2571, e-mail: Richard.Meyer@dlr.de

using morphological functions.

To be regarded as contrails, the resulting objects additionally have to consist of more than 10 pixels, must be longer than 15 pixels and must fit to the actual filter direction applied.

The filtering and testing procedures are repeated for 16 directions and the results are added to a binary contrail array. The proposed scheme mainly marks contrails of a width of 1 or 2 pixels. To detect wider contrails the whole algorithm is then applied to images reduced by a factor of 2. The results of this step are again added to the final binary contrail mask.

The performance of this scheme was tested against interactive interpretations of 60 satellite images by two observers. Greatest errors are found at the off-nadir scene borders due to the reduced horizontal pixel resolution there. To diminish this effect only a scan-angle of $\pm$ 50°is used.

Accurate visual inspection by zooming and optimizing the contrast confirms the assumption that many actual contrails still are undiscovered by the algorithm. In spite of the normalization the automatic scheme with its fixed parameters is inferior to the human eye in adapting to the specific contrasts in parts of the image. Thus the observer is able to recognize many more mostly weak contrails. But contrail coverage from AVHRR-images derived by the trained observers differed by a factor of 2, which shows that visual inspection is highly subjective. With the used algorithm we reach a detection efficiency defined as the ratio of correct contrail detections to the amount of all visually recognized contrails of 30 % to 50 %.

3 RESULTS

The contrail detection algorithm is applied to AVHRR-images of NOAA-14 covering Central Europe (Fig. 1). We processed 660 daily noon scenes from April 1995 to February 1997. In Fig. 1) all remapped noon (1230 UTC $\pm$ 45 min) contrail masks are superimposed. It can be seen that the observed contrails accumulate mainly close to and in direction of the major flight routes.

Fig. 1) indicates that the algorithm is robust against misdetections of surface features. As you see coastlines and mountain ridges are almost never misclassified. Only Lake Balaton in Hungary seems to get falsely classified as contrail a few times. Therefore misdetections of static surface features and sensor line failures that are avoided through skillful parameter setting can be neglected for regional contrail cloud coverage.

To calculate the regional AVHRR-derived contrail coverage we divide the counts of the stacked contrail masks (Fig. 1) by the number of possible detections and filter the data with a circular gauss-kernel of 50 pixels. We have chosen this radius to represent the visibility range of a ground-based observer. Additionally the derived contrail cloudiness is corrected for yearly averaged inhomogeneity of the background. Like described by Mannstein et al. [7] this procedure adapts the reduced contrail detectivity to values which could be obtained above a thermally homogeneous background. Especially above more heterogeneous surfaces like land the AVHRR-derived corrected contrail coverage ccc gets enforced. This strong dependence of detection efficiency on $\overline{SDT5}$ is caused by normalizing the data.

Looking at the Alps in Fig. 1) we recognize that obviously above a certain value of $\overline{SDT5}$ we hardly can detect any contrails. As we cannot avoid this effect we exclude all pixels where $\overline{SDT5}$ exceeds 0.85 K (Fig. 2) from further considerations.

The average for the corrected daytime contrail coverage ccc in the whole dataset (Fig. 2) amounts to 0.5 % $\pm$ 0.25 %. The spatial pattern of the algorithm-derived contrail coverage agrees with the contrail observations by Bakan et al. [1]. They also obtained the maxima in the North-Atlantic flight corridor with declining contrail cloudiness to the Eastern and Southern parts of Europe. The absolute value for contrail cloudiness observed by Bakan et al. [1] is on the average 1.6 times higher than the annual mean of ccc we derived. This may be an effect of analyzing different years, but we also assume, that the deviations of absolute values may arise from the applications of two different methods. Again, this comparison indicates that trained human observers are more effective in contrail detection.

An advantage over the analysis of Bakan et al. [1] is the higher spatial resolution. Some heavily flown air traffic routes can still be recognized in Fig. 2). Maxima of contrail coverage of 1.0 % and higher are found over Wales, The Channel and in the Balaton region. The latter is as mentioned before partly caused by some misdetections occurring over Lake Balaton, but affects ccc just locally in a moderate way.

Fig. 3 shows the daily variation of the average contrail coverage in the area between 0°E and 20°E, 48°N and 55°N. To derive values comparable to Fig. 2) we applied the heterogeneity-correction using the annual average of $\overline{SDT5}$ for this box. Thereafter, the daily contrail coverage ccc varied from 0.0 % up to 5.7 % with a standard deviation of 0.6 %. Because contrails themselves lead to enhanced heterogeneity in the temperature images, we did not take into account the actual $\overline{SDT5}$ of the analyzed scene for heterogeneity-correction. But, avoiding this positive feedback on ccc we do neglect reduced detection efficiency caused by other image features.

As the 30-d floating average in Fig. 3 suggests, there are remarkable annual variations with a ccc-minimum below 0.2 % during summer and a ccc-maximum close to 0.9 % during winter and spring. But annual variations of detection efficiency might have influenced the results.

Additionally we analyzed NOAA-14 night scenes (0145 UTC $\pm$ 50 min) for the midseason months. With regard to the higher detection efficiency during night we used the nocturnal $\overline{SDT5}$-images for the heterogeneity correction. We found a mean nighttime contrail coverage ccc of 0.24 %, while ccc for the same period on daytime was 0.70 % (Fig. 3). Thus contrail coverage at night is about one third of the daytime noon coverage.

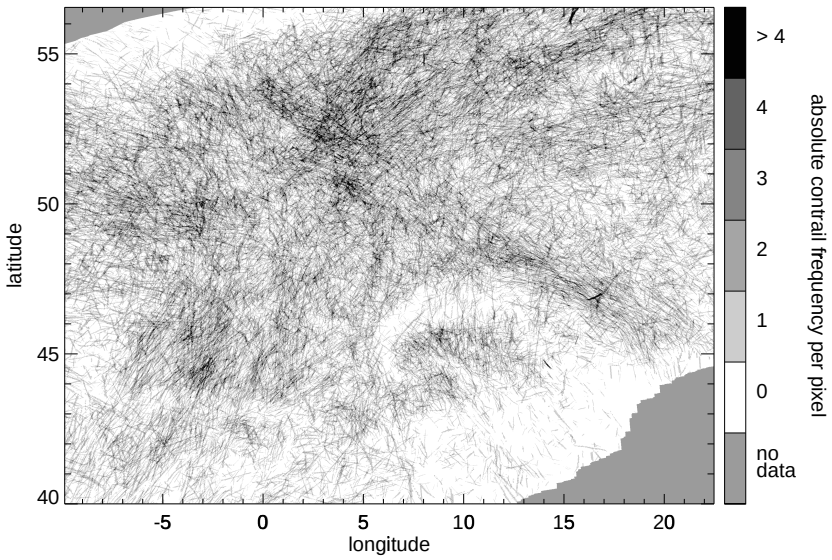

Figure 1: *Superimposed contrail masks for the period March 1995 to February 1997 (derived from 660 AVHRR passages 1230 UTC $\pm$ 45 min, pixels with less than 50 passages marked as "no data").*

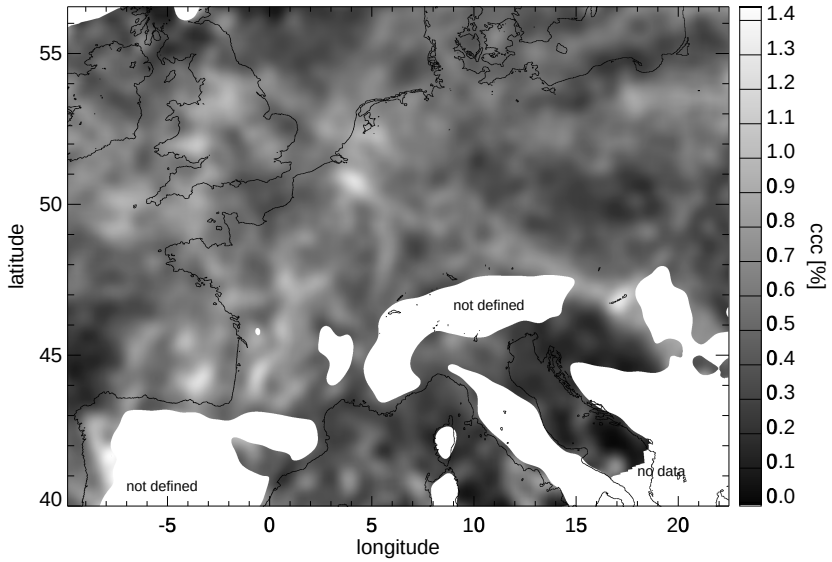

Figure 2: *Annual AVHRR-derived heterogeneity-corrected contrail coverage ccc derived from Fig. 1 ("not defined" are pixels with $\overline{SDT5} > 0.85$ K).*

4 Conclusions

The mean of the heterogeneity-corrected AVHRR-derived contrail coverage ccc reached 0.5 % $\pm$ 0.25 % over Western Europe. We recognize strong temporal and spatial variations in contrail coverage which match those derived by Bakan et al. [1]. Absolute values derived here are smaller by a factor of 1.6 which is of low significance due to analysis of different time-periods. Large differences of the two investigations can also be explained by an overestimation of the visual interpretations, but also by the poor detection efficiency of the automated scheme.

For the midseason month within this period we derive a nighttime contrail coverage of 0.2 % which has to be compared to 0.7 % for the same period from AVHRR-noon-passages. The observed annual cycle has its maxima during winter and spring, but might still be influenced by a differing detection efficiency.

Beyond this the scheme is not able to detect atypical contrails such as very wide spread and fuzzy ones, which are hard to distinguish from natural cirrus. The approach used also cannot recognize cases where

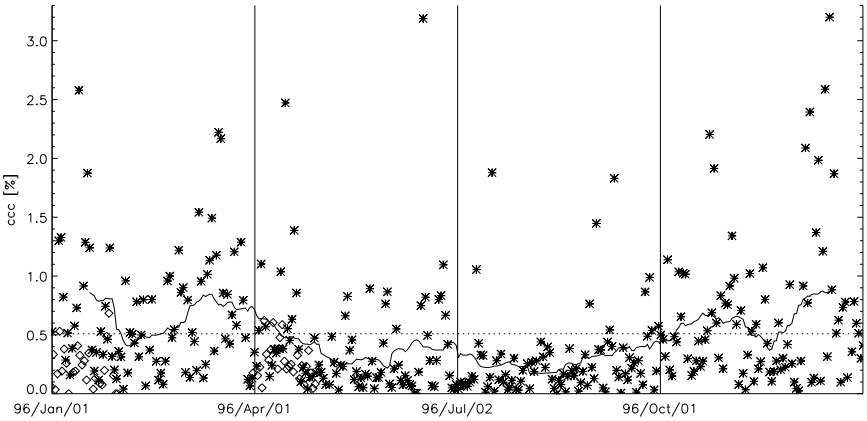

Figure 3: *Average AVHRR-derived corrected contrail coverage ccc for the box 0°E to 20°E, 48°N to 55°N. Asterisks are noon passages, diamonds nighttime passages. The solid line shows the 30-d floating average, the dotted line marks the annual average for daytime. Plotted are all values where data coverage was higher than 70 %. Not shown: absolute maximum of 5.6 % at January 14th 1996.*

contrails cover a large proportion of the sky destroying their individual line pattern.

Automated contrail recognition gives the opportunity to derive contrails' optical properties and their cloud forcing which should be further investigated to clearly define what kind of contrail are recognized by the automatic scheme.

Acknowledgments: This work was supported by BMBF (German Fed. Min. for Education, Science, Research and Technology) and the Bavarian State Min. for Reg. Development and Environmental Affairs.

REFERENCES

[1] S. Bakan, M. Betancor, V. Gayler, and H. Grassl. Contrail frequency over Europe from NOAA-satellite images. *Ann. Geophys.*, 12:962–968, 1994.

[2] M. Betancor Gothe and H. Grassl. Satellite remote sensing of the optical depth and mean crystal size of thin cirrus and contrails. *Theor. Appl. Clim.*, 48:101–113, 1993.

[3] M. Engelstad, S. K. Sengupta, T. Lee, and R. M. Welch. Automated detection of jet contrails using the AVHRR split window. *Int. J. Remote Sensing*, 13(8):1391–1412, 1992.

[4] J.-F. Gayet, G. Febvre, G. Brogniez, H. Chepfer, W. Renger, and P. Wendling. Microphysical and optical properties of cirrus and contrails: cloud field study on 13 october 1989. *J. Atmos. Sci.*, 53:126–138, 1996.

[5] M. Kästner, K. Kriebel, R. Meerkötter, W. Renger, G. Ruppersberg, and P. Wendling. Comparison of cirrus height and optical depth derived from satellite and aircraft measurements. *Mon. Wea. Rev.*, 121:2708–2717, 1993.

[6] K. N. Liou. Influence of cirrus clouds on weather and climate processes: a global perspective. *Mon. Wea. Rev.*, 114:1167–1198, 1986.

[7] H. Mannstein, R. Meyer, and P. Wendling. Operational detection of contrails from NOAA-AVHRR-data. *Int. J. Remote Sensing*, submitted, 1998.

[8] P. Minnis, J. K. Kirk Ayers, and S. P. Weaver. Surface-based observations of contrail occurrence frequency over the U.S., April 1993 - April 1994. Ref. Pub. 1404, NASA, June 1997.

[9] P. Minnis, D. Young, L. Nguyen, D. Garber, J. Smith, W.L., and R. Palikonda. Transformation of contrails into cirrus during success. *Geophys. Res. Lett.*, SUCCESS Special Issue, submitted June 1997, 1998.

[10] U. Schumann. On the effect of emissions from aircraft engines on the state of the atmosphere. *Ann. Geophys.*, 12:365–384, 1994.

[11] U. Schumann. On conditions for contrail formation from aircraft exhausts. *Meteor. Z.*, 5(3):4–23, 1996.

[12] U. Schumann and P. Wendling. Determination of contrails from satellite data and observational results. In U. Schumann, editor, *Lecture notes in engeneering: Air traffic and the environment - background, tendencies and potential, DLR international colloquium, Bonn, Germany, November 15/16, 1990, 140-153*, volume 60, 1990.

[13] B. Strauss, R. Meerkoetter, B. Wissinger, P. Wendling, and M. Hess. On the regional climatic impact of contrails – microphysical and radiative properties of contrails and natural cirrus clouds. *Ann. Geophys.*, in press, 1997.